International Journal of Engineering Trends and Technology
ISSN: 2231–5381 / https://doi.org/10.14445/22315381/IJETT-V72I9P115

Volume 72 Issue 9, 184-196, September 2024

Original Article

An Experimental Investigation of Solar Nano Fe_3O_4 Coating Exhibiting Higher Solar Absorption Efficiency using Box- Behnken Design

Markndeyulu Vuggirala[1], N. Alagappan[2], CH V K N S N Moorthy[3*], N.V.Narasimrao rao[4]

[1,2,4]*Department of Mechanical Engineering, Annamalai University, Annamalai Nagar, Chidambaram, Tamil Nadu, India.*
[3]*Vasavi College of Engineering, Ibrahimbagh, Hyderabad, Telangana State, India.*

**Corresponding Author : krishna.turbo@gmail.com*

Received: 21 May 2024 Revised: 08 August 2024 Accepted: 02 September 2024 Published: 28 September 2024

Abstract - *This paper presents a study that explores the use of nanocoating on a flat plate collector to enhance heat transfer in a conventional flat-plate solar water heater through an experimental approach. Globally, people are facing an increasingly serious energy dilemma. Numerous studies employing replenishable energy sources, such as sun energy as opposed to fuel and electrical energy, are conducted in an effort to control the energy crisis issue. This is because solar energy is free of cost and environmentally benign. Several research studies have tried to improve the effectiveness of solar water heaters. A simple and effective method of utilizing solar power is to warm water for household purposes. Despite the significant upfront expense of a solar water heating system, there are no ongoing green energy costs. The coating is created by integrating a metallic particle, fe3o4, into the black paint. With variations in ratios (1g, 1.5g, and 2g) were applied on three distinct flat plate collectors. Throughout this research, efficiency was evaluated for fe_3o_4 nanocoating and keeping flat plate collectors at varying tilt angles (15°, 30°, and 45°) and diverse flow rates (60, 90, and 120 kg/hr).*

Keywords - *Collector performance, Heat transfer fluid, Optimum angle, Optimum flowrate, Selective surface coatings.*

1. Introduction

An enormous heating load is turned on during peak hours, exacerbating the already existing imbalance between supply and demand for power. Considerable progress can be made in closing the gap if the heating load is shifted from conventional to non-traditional energy sources. Being completely free to operate, solar energy is the most efficient renewable energy source available. It may also close the gap between supply and demand for electricity, saving money. Many applications needing fluid temperatures lower than 80˚C use flat plate collectors, including space heating and household hot water. A straightforward and efficient technique to use solar energy is to heat water for household use. One variety of solar thermal collectors is [1]. Collector outcome is calculated [2]. The study was carried out in Bangladesh, with a 12-month data collection period. It has been discovered that the FPC water heater can operate continuously [3, 4]. The working fluid in the paper is suggested to be a phase transition material. At a certain temperature, it goes through a phase transition and releases latent heat, which heats the water. It is recommended. [5] It is suggested that the collecting mount be tilted weekly, seasonally, or biannually rather than leaving it in place all year. Finding out the long-term effectiveness of the FPC using the system advisor model is the goal of the experiment.[6]. [7] In this research, two FPCs are examined: one has a traditional design, and the other has a novel design, meaning that in this collector, heat transmission occurs directly from the absorber plate to the fluid. Additionally, GI is employed in place of Cu for the absorber plate material. Additionally, choosing a different collector results in a slight change in the output temperatures. An experiment is conducted [8], and the findings show that the water heater's efficiency is dependent on the flow rate through the collector; as the flow rate and incident solar radiation increase, so does the collector's efficiency. The effectiveness of a solar water heater is increased in this research [9] by heating an auxiliary tank that holds cold water in front of the sun and then moving it inside to heat the water quickly. This research [10] examines several incentives that might be provided to customers in order to encourage them to use solar water heaters more often. A study was conducted to analyze the V-Through Flat Plate Collector experiments conducted in Rajasthan's hot climate. One case study pertaining to this effort in Jaipur has been presented in this. The effectiveness of the solar flat collector has been observed to be enhanced by the V-grooved reflector. The research work on the effectiveness improvement of the solar water heater. In this, the zigzag grooves and three layers of

glass were used in the absorber plate to analyze the performance of solar flat collectors. The results show that the performance of flat plates shows enhanced in overall conditions. The effectiveness of various tube arrangements for solar water heating systems was researched. Increasing various tube arrangements' thermal efficiency.

The high percentage of heat gathered in a zigzag tube layout in both the summer and winter seasons. Hot water is released after the water, which enters from the plate's bottom side, is heated up in the collector area. Among unconventional energy sources, solar energy is the most efficient. In the realm of green energy, solar power is becoming increasingly favoured because it is suitable for heating water in both residential and commercial settings. This is because fossil fuels, such as gas and oil, are becoming more and more expensive. By calculating the instantaneous efficiency values for various variables, the thermal efficiency of the solar collector was ascertained. A work review on current efforts to improve the efficiency of solar water heaters.

The primary emphasis of this study is the most recent advancements in the field of Solar Water Heaters (SWH). The research focuses mostly on the application of several strategies integrated to enhance solar water heater performance. These solar systems' performance is collector-dependent. The water is heated using the heat that the collector captures from the sun to the greatest extent possible. There are numerous tiny solar water heater designs available today. Solar water heaters frequently employ thermal performance-enhancing approaches, including the use of rough or grooved surface absorbers. P. Shivkumar In this investigation, the results demonstrate that the efficiency increases with the number of riser tubes and that these riser tubes are arranged in a zigzag pattern or Z configuration. Currently, this device outperforms the traditional flat plate collector in terms of efficiency. A solar system may provide 7 kW/m2 of heat in a single day. Solar energy is frequently actively converted into heat using solar collectors. A naturally occurring solar thermal technology is the sunwater heating system. Heat is produced by incident solar radiation in solar water heating systems and is then transferred to a transfer medium, like water. It is frequently feasible to replace energy and fossil fuels used for water heating with solar water heating.

2. Literature

The sun is the primary source of energy for most terrestrial sources. The sun produces 1.8 x1015 TW of energy or more than 99.9% of all energy sent to Earth today. Every day, our planet receives electricity from the sun's rays, which is a million times more than the total energy generated by all of Earth's power plants combined. Therefore, we cannot anticipate a worldwide energy crisis brought on by the sun, yet solar energy is 20,000 times more powerful than what we currently utilize. Given that there is no pollution or environmental harm associated with its usage, this quantity appears to be a great source for meeting human requirements [9–11]. Bostrom and associates published research on nickel alumina coatings made from thermal solar absorber solutions in 2007. The ideal coating parameters were determined to be a molecule size of 10 nm, a thickness of 0.1 m, and a concentration of 65% nickel.

The permeable layer comesto a typical warm conductanc e of 0.03 and an ordinary sun-powered absorbance, sol, of 0.83. By adding an antireflection layer to the introduction retaining layer, the absorber's execution was advanced. The sample with the best antireflection coating achieved a thermal emittance of 0.04 and a solar absorptance of 0.93[12-19]. Katumba et al. (2008) investigated how carbon nanoparticles incorporated in SiO2, ZnO, and NiO matrices prepared by the solgel technique functioned as solar selective absorbers.[14]. Aluminium substrates were used for testing the coatings. Thermal emissivity and solar absorption can be determined through UV, VIS, and FTIR spectroscopy to ascertain the spectral response of composite coatings. The samples of the NiO matrix showed the best solar selective behaviour, and they suggested a theoretical evaluation framework for more material comparisons of this type. The study "Comparison between aesthetic and thermal performances of copper oxide and titanium dioxide Nano particulate coatings" was conducted by Mehdi Baneshi et al. in 2011.

The authors presented a brand-new optimization technique for creating coloured coatings that takes into account both aesthetic and thermal consequences. PVD-deposited solar selective coatings with high absorptance and low emittance have been thoroughly investigated. This study paper includes a detailed description of PVD coatings that are commercially available for use in flat plate solar thermal power production applications.

In contrast to the conventional black paint coating, Ehab AlShamaileh (2010) proposed a selective coating with a higher solar absorption efficiency for the black paint based on a nickel-aluminum (NiAl) alloy. A mass percentage of 6% NiAl alloy was the ideal composition. It is clear from the talk above that a large number of motivated researchers have used nanomaterials in numerous experiments and published their results. The studies' overall conclusion is that nanomaterials, such as chromium particles with black paint, cupric oxide, SiO2, ZnO, NiO matrices, and Ni-Al alloy, are significant.

2.1. Box-Behnken Design

For the response surface approach, the Box-Behnken design works well because it allows for the following tasks:

- Estimating the quadratic model's parameters.
- Creating sequential designs.
- Using blocks
- Identifying instances where the model does not suit the data.

Response surface designs, such as the Doehlert matrix, Box-Behnken design, and three-level full factorial design, are contrasted with one another. According to the findings, the central composite design is only slightly more efficient than the Doehlert matrix and Box-Behnken design, which are both much more efficient than the three-level complete factorial designs.

3. Experimental Procedure

The temperature coupling points and the schematic diagram of the tank under discussion and the solar flat collector are shown in Figure 1. The flat plate collector is situated next to a 100-liter tank and is inclined north and south. A 2.0 m^2 flat plate collector with nine riser tubes with an outer diameter of 1.27 cm, each measuring 6 feet in length and 1.2 cm in wall thickness, makes up the experiment portion. Copper heat-collecting surfaces with a 0.20 mm thickness make up these riser tubes. Using thermocouples installed alternately on riser pipes, the wall temperature distribution of the collection plate riser pipe was measured. Moreover, the water's temperature is increased.

3.1. Specification of Flat Plate Collector

- Flat plate collector area = 1.8 m^2
- Two glass covers of 4 mm thickness are provided with pads. The absorber is tube and sheet type.
- Number of tubes = 9Tubes dimensions
- outer diameter = 10 mm
- Wall thickness = 1 mm
- Long = 2m (9 tubes of 10 mm ODI mm wall thickness and 2m long are equispaced, and 75mm width corrugated black painted fins are embedded over the tube).
- The bottom and top headers' outer diameter = 25 mm.
- Black paint is used to coat the absorber.
- 50 mm thick mineral wool insulation is used below the absorber and around the edges.

On an absorber plate, the collector was tested using a selective coating of commercial black paint mixed with fe_3o_4 at several ratios (1%, 1.5%, and 2%). and maintaining the collector at three distinct tilt angles: 300, 450, and 600. The collector utilized in this project is 1 x 1.2 m in size, with a copper thickness of 2 mm. It has nine copper tubes evenly distributed on it, each measuring 10 mm on the outside and 9 mm on the inside. The input and outlet headers, which have a diameter of 60 mm, were tested under various solar radiation conditions and collector tilts. The working substance, water, was tested at various flow rates, with varying Fe_3O_4 coating ratios on three collectors and at various tilt angles. Thermos couples are positioned in different places, as shown in the figure 2.

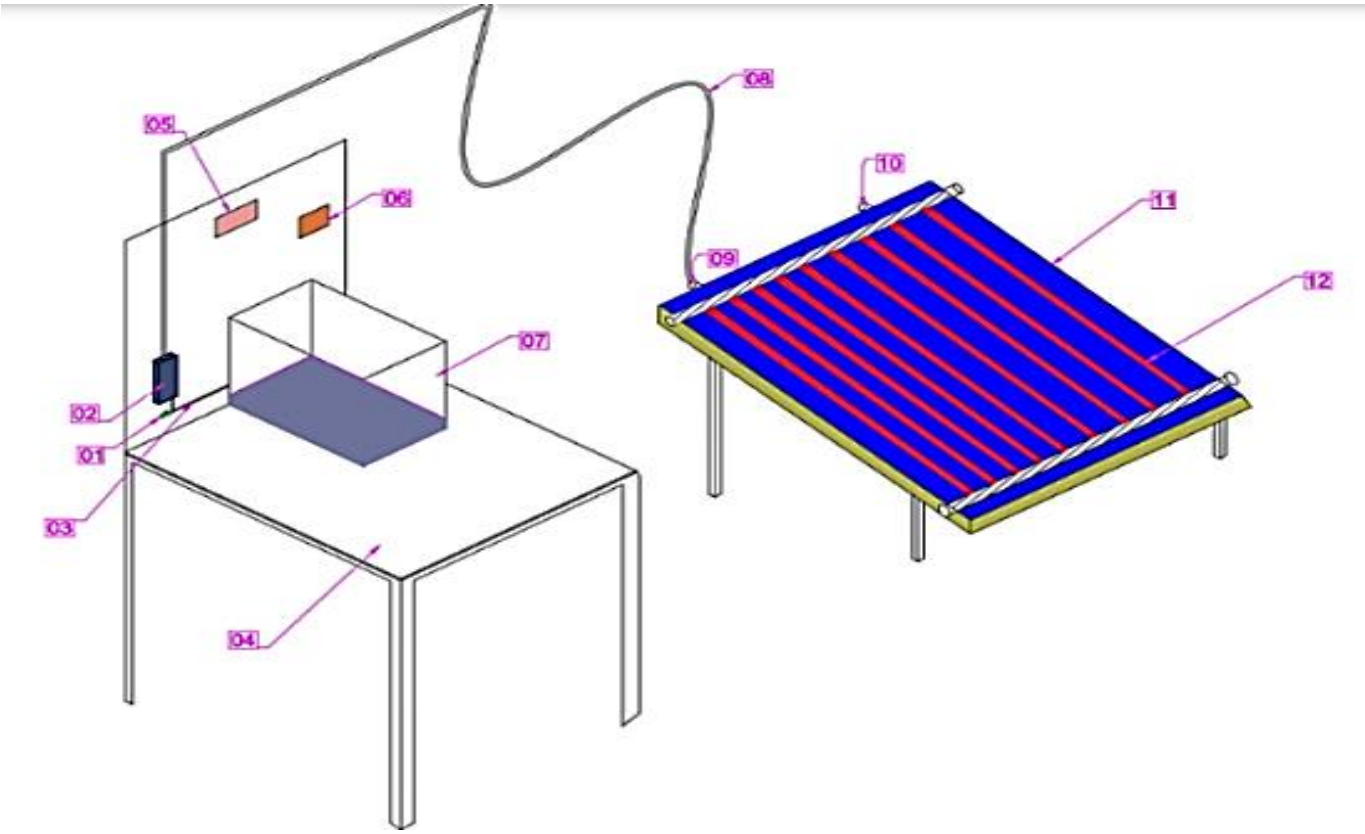

Fig. 1 Experimental setup (1) External Motor, (2) Rotameter, (3) Pipe, (4) Table, (5) Digital Temperature Indicator, (6) Thermocouple nob, (7) Water Tank, (8) Water Pipe Connected To Collector, (9) Inlet Value, (10) Out Value, (11) Absorber Plates, (12) Copper Tubes.

3.2. Collectors with Nanocoating

collector **C1** coated with 1g of Fe_3O_4 in commercial black paint.

collector **C2** coated with 1.5g of Fe_3O_4 in commercial black paint.

collector **C3** coated with 2g of Fe_3O_4 in commercial black paint.

Fig. 2 Collectors coated with nano particulars with different ratios

3.3. Data Reduction

Thermal efficiency is the ratio of heat output to heat input. The thermal efficiency (η%) of the FPC is computed using

3.3.1. Heat gain by the Cold Fluid or Useful Energy

$$Q_c = m_c C_{pc} (\Delta T) \text{ watts}$$

m_c = Mass flow of cold fluid kg/s

C_{pc} = Specific heat of cold fluid = 4186.8 j/kg-k.

3.3.2. Heat Energy absorbed by the Collector

$Q_a = I \times A$ watts

I = Intensity of solar radiation in w/m^2

average solar power in India is 5kw

but I = 5 cos α (α= angle of tilt)

FPC Surface Area of Collector = $0.1 \times 2 = 0.2\ m^2$

Total collector area (A) = Surface area x number of tubes (n) $A = 0.2 \times 9 = 1.8\ m^2$

3.3.3. Efficiency of the unit

$$(\eta\%) = \frac{Qc}{Qa} \times 100$$

3.4. Expected Outcomes

It is suggested that fe_3o_4 nanoparticles be mixed with black paint from the store, put on an absorber plate, and selected for additional research that will result in analysis, both theoretical and experimental, which may show gains in the collector's functionality.

- It is anticipated that nanoparticles will increase absorption capacity.
- The absorber's emissivity and absorbtivity will both benefit from nano coatings.
- It is expected that the metallic-coated collector's operating fluid will warm up more at the output.
- Cost reduction may be possible with nanocoatings.

3.5. Process Parameters and their Levels

Table 1. Process parameters

Parameters	Levels		
	-1	0	1
Flow rate(kg/hr)	60	90	120
Angle (degrees)	15	30	45
Concentration (grams)	1	1.5	2

3.6. Design of Matrix

The Design of Experts (DOE) is a useful tool for organizing experiments and efficiently analyzing the collected data.

The choice of the input variables and the response (output) that will be measured is the first step in the experimental task. BBD produced 17 simulation runs for a copper-absorbed plate with a Fe_3O_4 nanocoating, grouped by three factors, as shown in Table 2.

4. Results And Discussions

4.1. ANOVA for Quadratic model

Response 1: Efficiency

Transform: Square Root

Constant: 0

Table 2. Design of matrix

Std	Run	Factor 1 A: flowrate Kg/hr	Factor 2 B: angle Degrees	Factor 3 C: concentration Grams	Response 1 Efficiency %	Response 2 Qa	Response 3 Qc
1	7	60	15	1.5	28.35	8.6931	2.46436
9	4	90	15	1	28.77	8.6931	2.5006
11	17	90	15	2	28.77	8.6931	2.5006
7	14	60	30	2	31.62	7.79418	2.46436
3	5	60	45	1.5	34.17	6.3639	2.17444
5	8	60	30	1	34.87	7.79418	2.71805
16	6	90	30	1.5	40.45	7.79418	3.15293
17	9	90	30	1.5	40.45	7.79418	3.15293
14	10	90	30	1.5	40.45	7.79418	3.15293
13	11	90	30	1.5	40.45	7.79418	3.15293
15	15	90	30	1.5	40.45	7.79418	3.15293
6	1	120	30	1	42.99	7.79418	3.35048
2	3	120	15	1.5	45.24	8.6931	3.93317
10	13	90	45	1	46.13	6.3639	2.93549
4	12	120	45	1.5	50.36	6.3639	3.20481
8	16	120	30	2	54.2	7.79418	4.22452
12	2	90	45	2	58.09	6.3639	3.69654

Table 3. ANOVA Table for Efficiency (Response 1)

Source	Sum of Squares	df	Mean Square	F-value	p-value	
Model	5.75	9	0.6394	3.74	0.0481	Significant
A-flow rate	3.22	1	3.22	18.81	0.0034	
B-angle	1.56	1	1.56	9.13	0.0194	
C-concentration	0.7354	1	0.7354	4.30	0.0769	
AB	0.0489	1	0.0489	0.2859	0.6094	
AC	0.0538	1	0.0538	0.3143	0.5926	
BC	0.0366	1	0.0366	0.2138	0.6578	
A^2	0.0253	1	0.0253	0.1478	0.7120	
B^2	0.0543	1	0.0543	0.3173	0.5908	
C^2	0.0249	1	0.0249	0.1455	0.7142	
Residual	1.20	7	0.1711			
Lack of Fit	1.20	3	0.3993	5.649E+07	< 0.0001	
Pure Error	2.828E-08	4	7.069E-09			
Cor Total	6.95	16				

Factor coding is Coded.

Sum of squares is Type III – Partial.

The significance of the model is indicated by its F-value of 3.74. This great of an F-value is 4.81% likely to be the result of noise. Model terms with P-values less than 0.0500 are deemed significant. In this case, A and B are significant model terms. If the value is greater than 0.1000, the model terms become irrelevant. If your model has many unimportant model terms (aside from those required to maintain hierarchy), model reduction may help improve your model. The Lack of Fit F-value of 56486601.23 suggests that the lack of fit is significant. Noise is likely to be the cause of a high Lack of Fit F-value by 0.01%. Since we need the model to fit, a notable lack of fit is not what we want. A poor Predicted R2 suggests

that rather than using the current model, the overall mean would be a more accurate predictor of your answer. A higher-order model might occasionally make superior predictions as well. Adeq Precision determines the signal-to-noise ratio. The ratio ought to be more than 4. You have a sufficient signal strength with a ratio of 6.930. This idea can be used to navigate the design space. The coefficient estimate, with all other factors maintained constant, shows the estimated change in response for each unit change in factor value. The total average response across all runs is the intercept in an orthogonal design. The coefficients show how the factor selections affected the modifications made in reference to that average. The VIFs are 1 when the factors are orthogonal, while multi-collinearity is indicated by any value higher than 1. The VIF increases with the strength of the factor relationship. It is common to think that less than ten VIFs are suitable. There are not any notable model terms here. If the values of the model terms are more than 0.1000, they are considered not significant. If your model has a lot of extraneous terms (apart from those required to maintain hierarchy), model reduction might be able to help.

Table 4. Fit Statistics

Std. Dev	0.4137	R^2	0.8277
Mean	6.34	Adjusted R^2	0.6062
CV %	6.52	Predicted R^2	-1.7567
		Adeq Precision	6.9300

Table 5. Coefficients in terms of coded factors

Factor	Coefficient Estimate	df	Standard Error	95% CI Low	95% CI High	VIF
Intercept	6.36	1	0.1850	5.92	6.80	
A-flow rate	0.6343	1	0.1463	0.2885	0.9801	1.0000
B-angle	0.4418	1	0.1463	0.0960	0.7877	1.0000
C-concentration	0.3032	1	0.1463	-0.0426	0.6490	1.0000
AB	0.1106	1	0.2068	-0.3785	0.5997	1.0000
AC	0.1159	1	0.2068	-0.3731	0.6050	1.0000
BC	0.0956	1	0.2068	-0.3934	0.5847	1.0000
A^2	-0.0775	1	0.2016	-0.5542	0.3992	1.01
B^2	0.1136	1	0.2016	-0.3631	0.5903	1.01
C^2	-0.0769	1	0.2016	-0.5536	0.3998	1.01

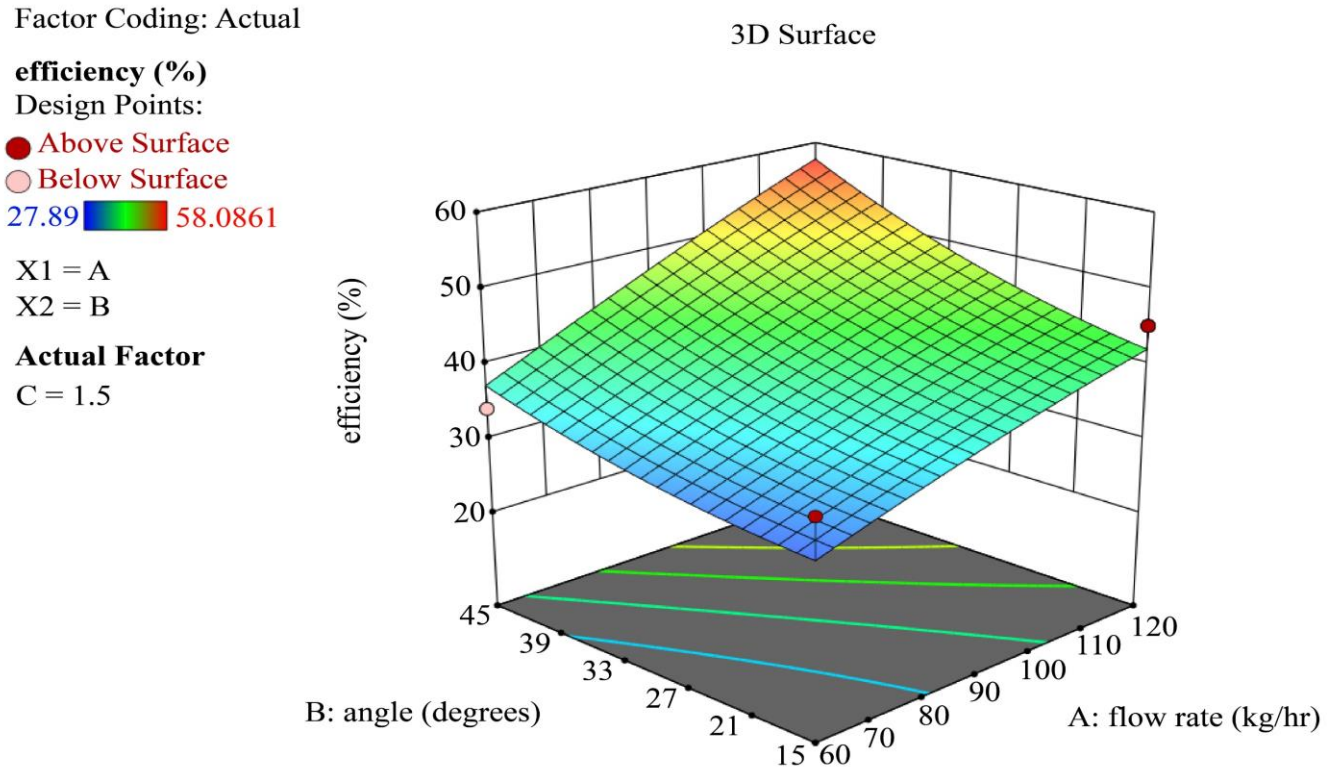

Fig. 3 Efficiency with Respect to angle and flow rate

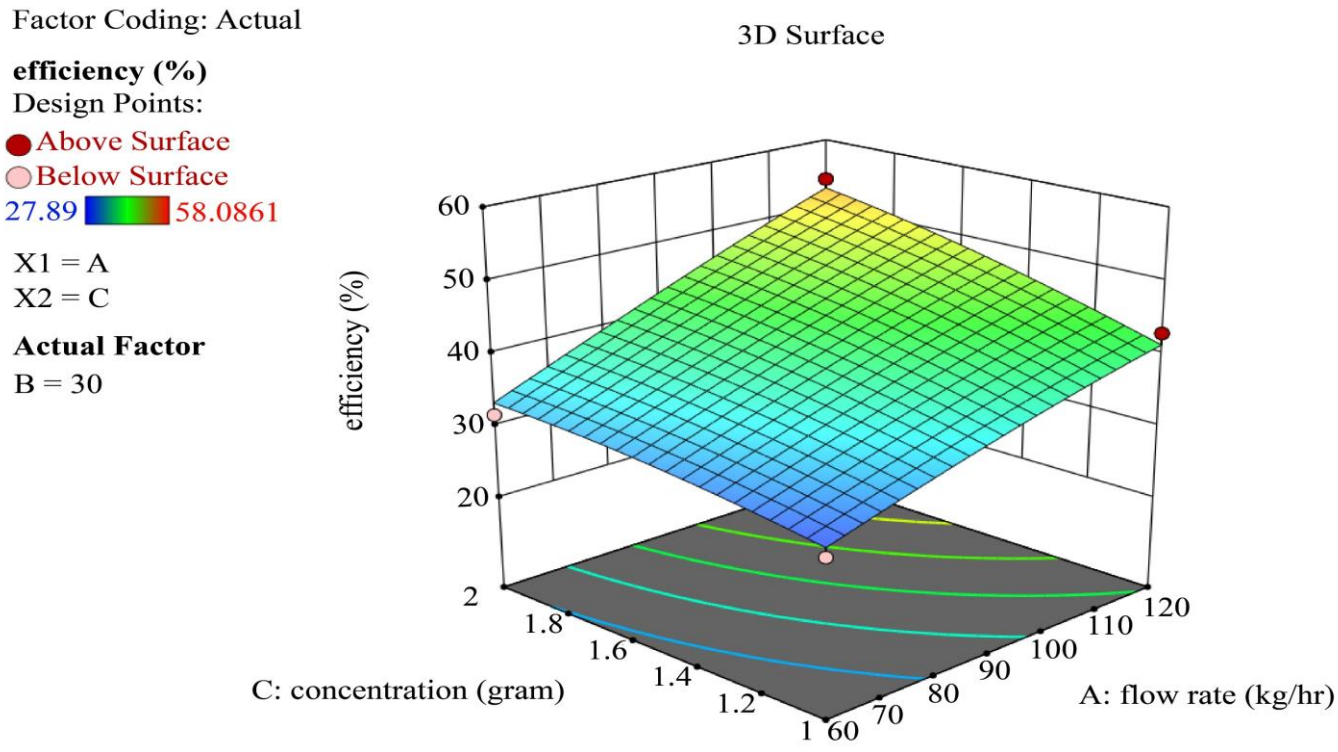

Fig. 4 Efficiency with Respect to concentration and flow rate

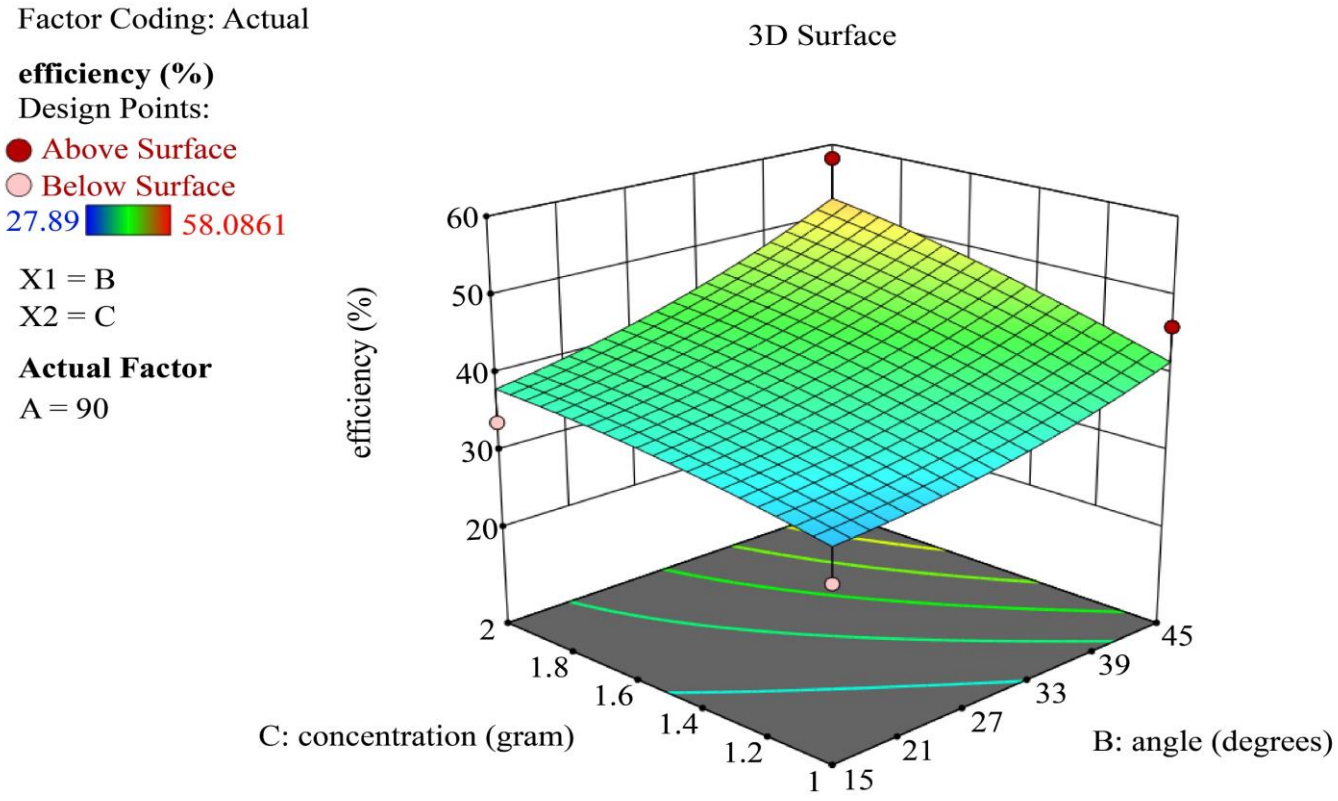

Fig. 5 Efficiency with Respect to concentration and flow rate

4.2. ANOVA for Quadratic Model

Response 2: Qa

Table 6. ANOVA Response for Qa

Source	Sum of Squares	df	Mean Square
Model	11.15	9	1.24
A-flow rate	0.0000	1	0.0000
B-angle	10.85	1	10.85
C-concentration	0.0000	1	0.0000
AB	0.0000	1	0.0000
AC	0.0000	1	0.0000
BC	0.0000	1	0.0000
A^2	0.0000	1	0.0000
B^2	0.2972	1	0.2972
C^2	0.0000	1	0.0000
Residual	0.0000	7	0.0000
Lack of Fit	0.0000	3	0.0000
Pure Error	0.0000	4	0.0000
Cor Total	11.15	16	

Factor coding is Coded.
Sum of squares is Type III - Partial.
P-values less than 0.0500 indicate that model terms are significant.

Table 7. Fit Statistics

Std. Dev.	0.0000	R^2	1.0000
Mean	7.67	Adjusted R^2	1.0000
CV %	0.0000	Predicted R^2	1.0000
		Adeq Precision	NA[(1)]

Table 8. Coefficients in Terms of Coded Factors

Factor	Coefficient Estimate	df	VIF
Intercept	7.79	1	
A-flow rate	0.0000	1	1.0000
B-angle	-1.16	1	1.0000
C-concentration	0.0000	1	1.0000
AB	0.0000	1	1.0000
AC	0.0000	1	1.0000
BC	0.0000	1	1.0000
A^2	0.0000	1	1.01
B^2	-0.2657	1	1.01
C^2	0.0000	1	1.01

There are no important model terms in this instance. The model terms are not important if the value is bigger than 0.1000. Model reduction could make your model better if it has a large number of unimportant model terms (apart from those needed to maintain hierarchy). Case(s) with a 1.0000 leverage: PRESS statistic and Pred R2 are not defined. There is less than 0.2 discrepancy between the Adjusted R2 of 1.0000 and the Predicted R2 of 1.0000, indicating a satisfactory agreement.When all other factors are maintained constant, the coefficient estimate shows the expected change in response for each unit change in factor value. The total average response of all the runs is the intercept in an orthogonal design. Based on the factor choices, the coefficients represent modifications made around that average. VIFs are 1 when the factors are orthogonal; VIFs more than 1 denote multi-colinearity; the higher the VIF, the stronger the factor connection. VIFs of fewer than 10 are generally acceptable.

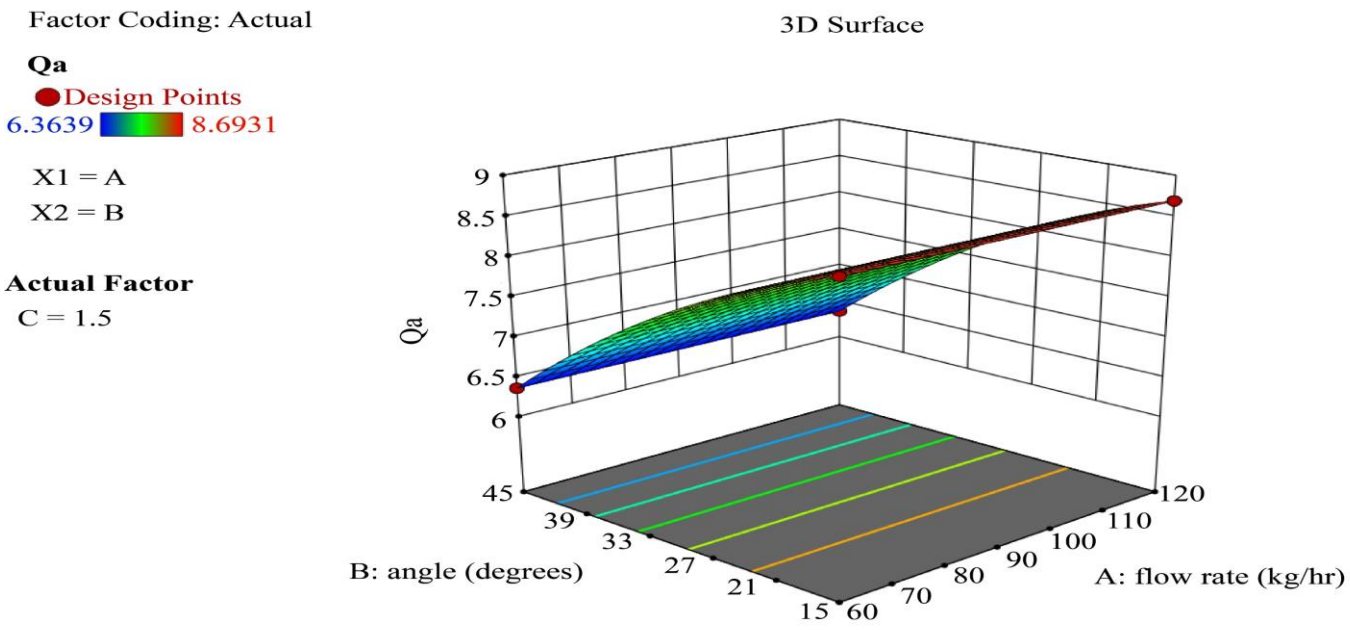

Fig. 6 Efficiency with Respect to angle and flow rate

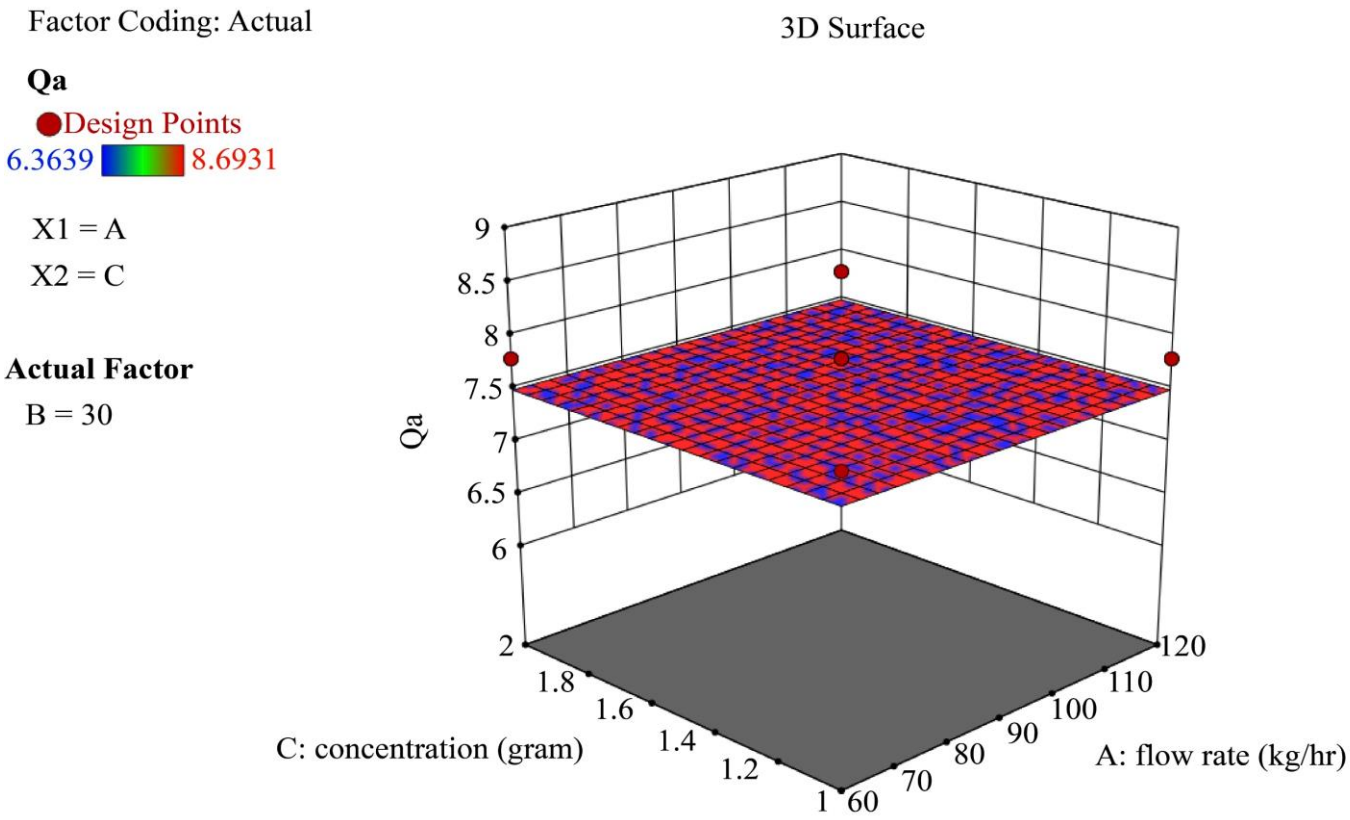

Fig. 7 Efficiency with Respect to concentration and flow rate

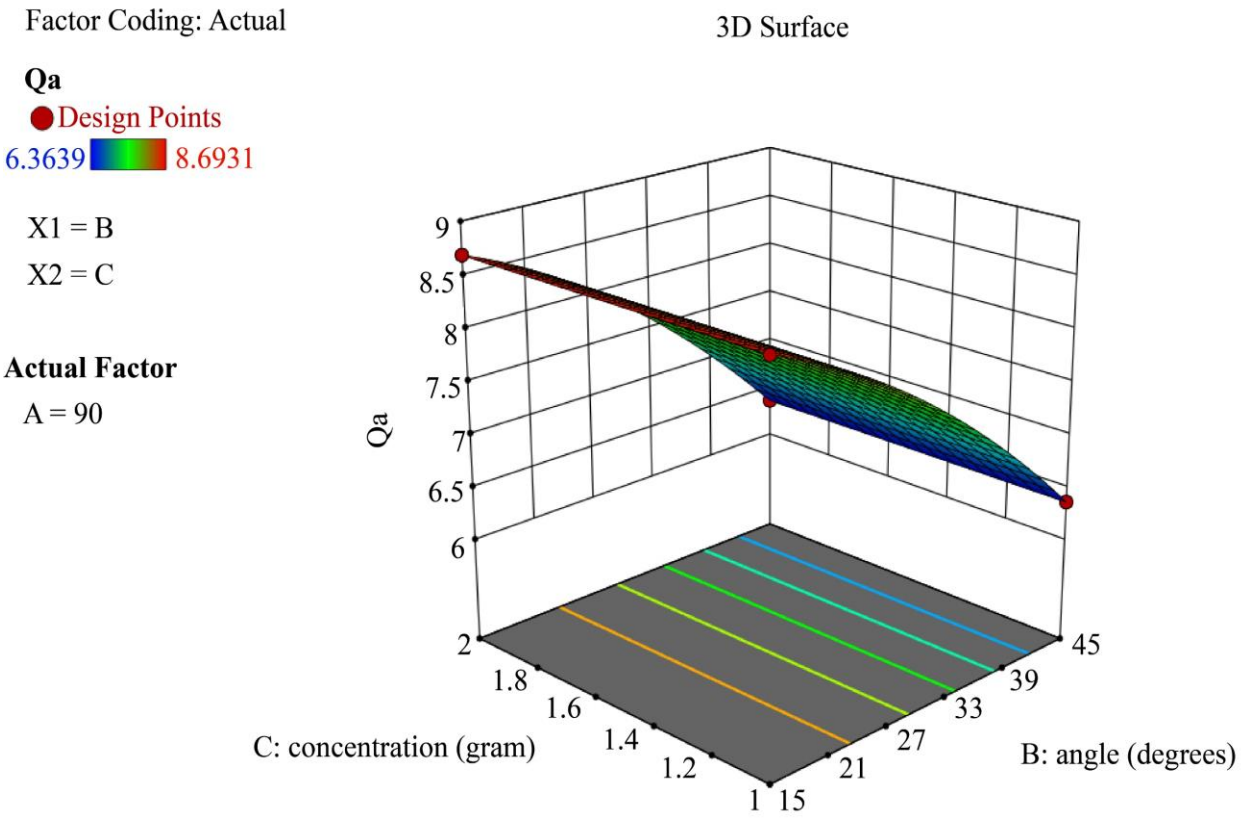

Fig. 8 Efficiency with Respect to concentration and flow rate

4.3. ANOVA for Quadratic Model

Response 3: Qc

Table 9. ANOVA Response for Qc

Source	Sum of Squares	df	Mean Square	F-value	p-value
Model	3.83	9	0.4251	2.69	0.1026
A-flow rate	2.95	1	2.95	18.66	0.0035
B-angle	0.0202	1	0.0202	0.1281	0.7310
C-concentration	0.6961	1	0.6961	4.41	0.0739
AB	0.0050	1	0.0050	0.0317	0.8638
AC	0.0853	1	0.0853	0.5402	0.4862
BC	0.0266	1	0.0266	0.1684	0.6938
A^2	0.0008	1	0.0008	0.0050	0.9457
B^2	0.0106	1	0.0106	0.0669	0.8033
C^2	0.0310	1	0.0310	0.1963	0.6711
Residual	1.11	7	0.1579		
Lack of Fit	1.11	3	0.3684		
Pure Error	0.0000	4	0.0000		
Cor Total	4.93	16			

Table 10. Fit statistics

Std. Dev.	0.3974	**R^2**	0.7759
Mean	3.08	**Adjusted R^2**	0.4877
CV %	12.89	**Predicted R^2**	-2.5862
		Adeq Precision	5.9190

Given the noise, the model's F-value of 2.69 suggests that it is not significant. A significant F-value like this has a 10.26% probability of being caused by noise. Model terms are considered significant when P-values are less than 0.0500. A is a significant model term in this instance. The model terms are not important if the value is bigger than 0.1000. Model reduction could make your model better if it has a large number of unimportant model terms (apart from those needed to maintain hierarchy).

According to predicted R2, the current model may not be as good at predicting your answer as the overall mean. A higher-order model might potentially be more predictive in some circumstances. Adeq Precision calculates the ratio of signal to noise. Ideally, the ratio should be higher than 4. With a ratio of 5.919, your signal strength is sufficient. The design space can be navigated using this concept. An unfavourable the predicted R^2 suggests that the current model may not be as good as the overall mean in predicting your answer. Higher-order models sometimes make better predictions as well. Adeq Precision is used for signal-to-noise ratio analysis.

An ideal ratio is greater than 4. Your ratio indicates a strong enough signal at 5.919. Use this model to navigate the design space. When all other factors are maintained constant, the coefficient estimate shows the expected change in response for each unit change in factor value. The total average response of all the runs is the intercept in an orthogonal design. Based on the factor choices, the coefficients represent modifications made around that average. VIFs are 1 when the factors are orthogonal; VIFs more than 1 denote multi-colinearity; the higher the VIF, the stronger the factor connection. VIFs of fewer than 10 are generally acceptable.

Table 11. Coefficients in terms of coded factors

Factor	Coefficient Estimate	df	Standard Error	95% CI Low	95% CI High	VIF
Intercept	3.15	1	0.1777	2.73	3.57	
A-flow rate	0.6069	1	0.1405	0.2747	0.9391	1.0000
B-angle	-0.0503	1	0.1405	-0.3825	0.2819	1.0000
C-concentration	0.2950	1	0.1405	-0.0372	0.6272	1.0000
AB	0.0354	1	0.1987	-0.4344	0.5052	1.0000
AC	0.1460	1	0.1987	-0.3238	0.6158	1.0000
BC	0.0815	1	0.1987	-0.3883	0.5513	1.0000
A^2	-0.0137	1	0.1936	-0.4716	0.4442	1.01
B^2	-0.0501	1	0.1936	-0.5080	0.4078	1.01
C^2	-0.0858	1	0.1936	-0.5437	0.3721	1.01

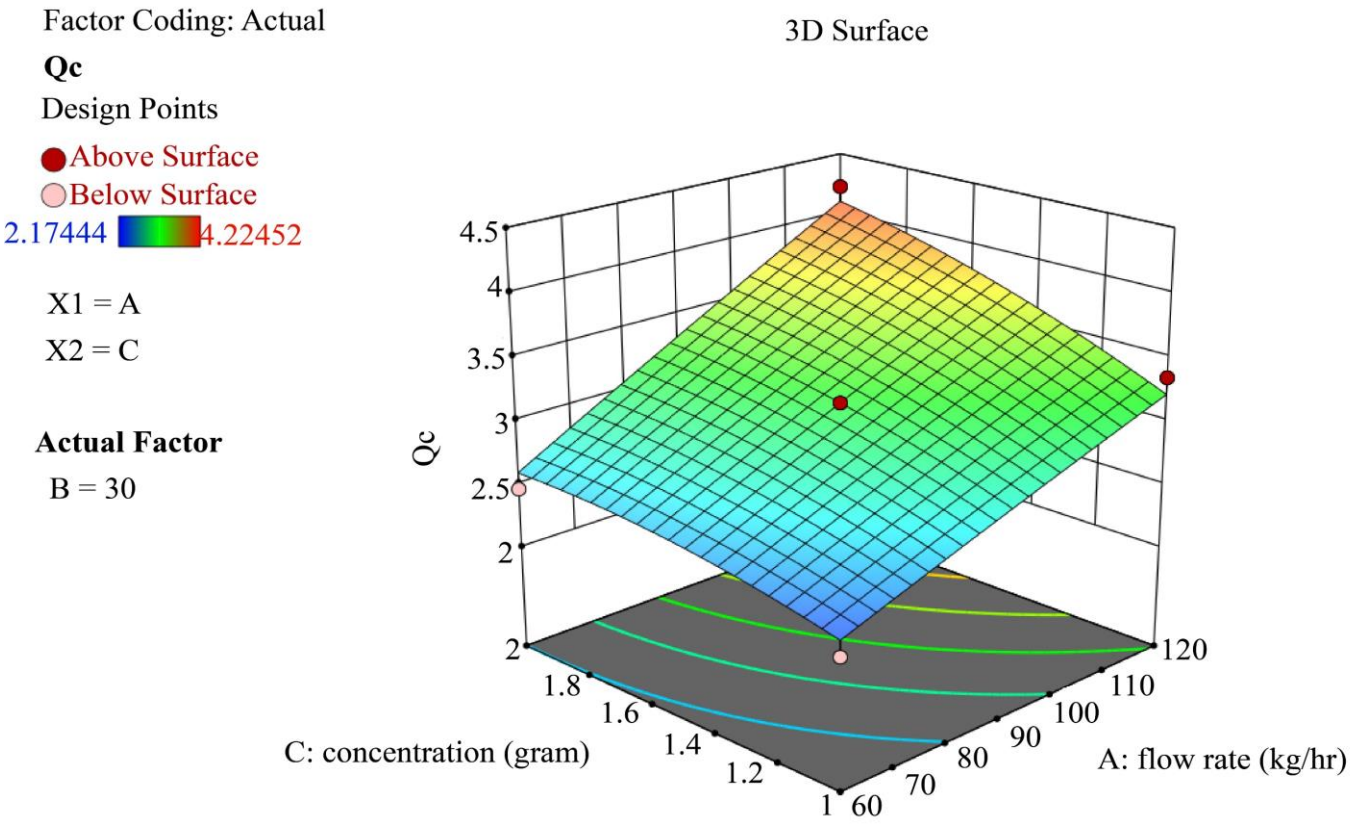

Fig. 9 Efficiency with Respect to concentration and flow rate

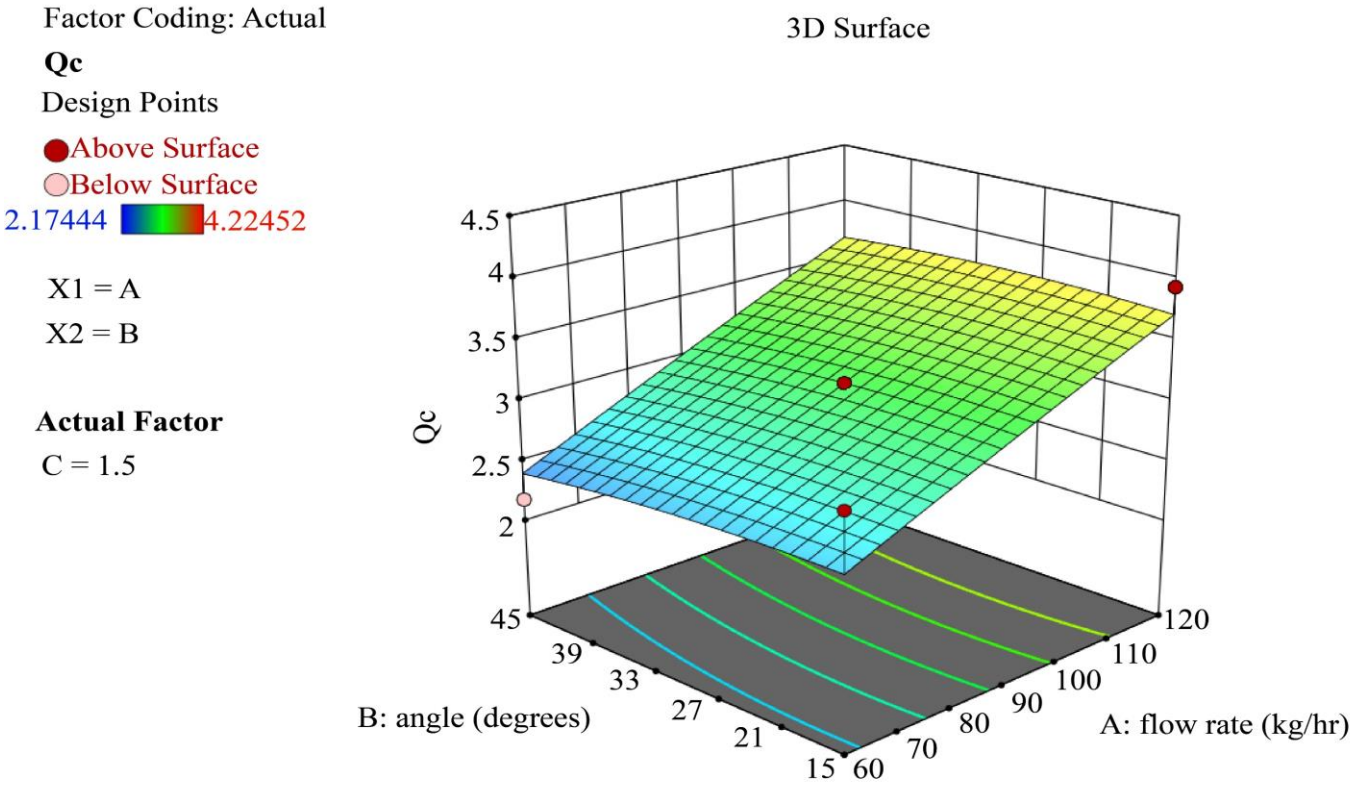

Fig. 10 Efficiency with Respect to angle and flow rate

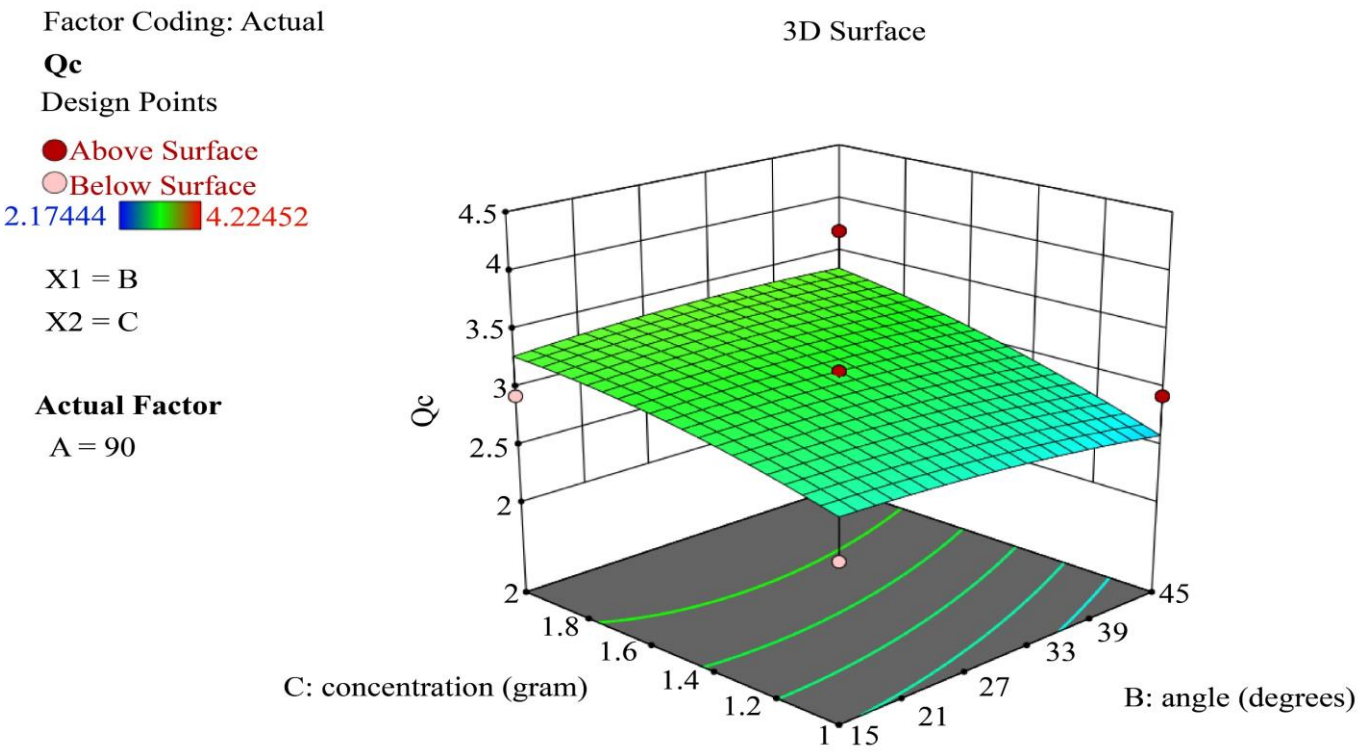

Fig. 11 Efficiency with Respect to concentration and angle

Nomenclature

BBD	-	Box-Behnken Design
Cu	-	Copper
ID	-	Inner Diameter
OD	-	Outer Diameter
RSM	-	Response Surface Methodology
DOE	-	Design of Experiments
FPC	-	Flat Plate Collector

RSM offers an accurate optimal location and is a helpful tool for optimizing parameters. Due to their simplicity, Box-Behnken and Central Composite designs frequently use RSM designs for parameter optimization and fitting second-order polynomials to response surfaces.

5. Conclusion

In order to increase absorptivity and decrease emissivity in a liquid flat plate solar water collector, this paper suggests using a variety of nanocoating techniques. It is a novel and cutting-edge approach in the field of solar systems that can be readily implemented at a reasonable cost.

Potential research results are discussed, along with the setup requirements for the experiment and the coating techniques for the nanomaterials. Based on the studies conducted, applying these nanocoatings to liquid flat plate collectors may significantly improve the solar collector's overall efficiency.

Experiments are carried out using BBD and assessed using Design of Experiments (DOE) software to assess the heat increase of copper absorbers employing nanocoating of Fe3O4. Comparing the SWHS to regular black paint from the store, it is evident that the new coating, which contains Fe3o4 particles, collects thermal energy more effectively. The above results were compared with experimental and RSM.

References

[1] Solar District Heating, SDH. [Online]. Available: http://www.solar-district-heating.eu/SDH/

[2] Jianhua Fan, Louise Jivan Shah, and Simon Furbo, "Evaluation of Test Method for Solar Collector Efficiency," *Proceedings of Eurosun,* Glasgow, UK, ISES-Europe, pp. 1-7, 2006. [Google Scholar] [Publisher Link]

[3] Jianhua Fan, Louise Jivan Shah, and Simon Furbo, "The Effect of the Volume Flow Rate on the Efficiency of a Solar Collector," *Proceedings of Eurosun,* Glasgow, UK, ISES-Europe, 2006. [Google Scholar] [Publisher Link]

[4] G.F. Jones, and Noam Lior, "Flow Distribution in Manifolded Solar Collectors with Negligible Buoyancy Effects," *Solar Energy,* vol. 52, no. 3, pp. 289-300, 1994. [CrossRef] [Google Scholar] [Publisher Link]

[5] Volker Weitbrecht, David Lehmann, and Andreas Richter, "Flow Distribution in Solar Collectors with Laminar Flow Conditions," *Solar Energy*, vol. 73, no. 6, pp. 433-441, 2002. [CrossRef] [Google Scholar] [Publisher Link]

[6] X.A. Wang, and L.G. Wu, "Analysis and Performance of Flat-Plate Solar Collector Arrays," *Solar Energy*, vol. 45, no. 2, pp. 71-78, 1990. [CrossRef] [Google Scholar] [Publisher Link]

[7] P.B. Rasmussen, and S. Svendsen, "Soleff Program for Calculation of the Efficiency of Solar Collectors," User Guide and General Program Documentation, Thermal Insulation Laboratory, Technical University of Denmark, 1996. [Google Scholar]

[8] P. Talebizadeh, M.A. Mehrabian, and M. Abdolzadeh, "Prediction of the Optimum Slope and Surface Azimuth Angles using the Genetic Algorithm," *Energy and Buildings,* vol. 43, no. 11, pp. 2998-3005, 2011. [CrossRef] [Google Scholar] [Publisher Link]

[9] Farzad Jafarkazemi, S. Ali Saadabadi, and Hadi Pasdarshahri, "The Optimum Tilt Angle for Flat-Plate Solar Collectors in Iran," *Journal of Renewable Sustainable Energy,* vol. 4, 2012. [CrossRef] [Google Scholar] [Publisher Link]

[10] Renewable Energy and Energy Efficiency Organization, 2021. [Online]. Available: http://www.satba.gov.ir/en/

[11] Umish Srivastva, R.K. Malhotra, and S.C. Kaushik, "Recent Developments in Heat Transfer Fluids Used for Solar Thermal Energy Applications," *Fundamentals of Renewable Energy and Applications*, vol. 5, no. 6, pp. 1-11, 2015. [Google Scholar] [Publisher Link]

[12] Mouna Hamed, Ali Fellah, and Ammar Ben Brahim, "Parametric Sensitivity Studies on the Performance of a Flat Plate Solar Collector in Transient Behavior," *Energy Conversion and Management*, vol. 78, pp. 938-947, 2014. [CrossRef] [Google Scholar] [Publisher Link]

[13] N. Madhukeshwara, and E.S. Prakash, "An Investigation on the Performance Characteristics of Solar Flat Plate Collector with Different Selective Surface Coatings," *International Journal of Energy and Environment*, vol. 3, no. 1, pp. 99-108, 2012. [Google Scholar] [Publisher Link]

[14] Ali Mohammad Noorian, Isaac Moradi, and Gholam Ali Kamali, "Evaluation of 12 Models to Estimate Hourly Diffuse Irradiation on Inclined Surfaces," *Renewable Energy*, vol. 33, no. 6, pp. 1406-1412, 2008. [CrossRef] [Google Scholar] [Publisher Link]

[15] Ali H. Assi, and M. Jama, "Estimation of solar radiation using sun hours in the Emirate of Abu Dhabi – UAE," *Proceedings of the 11th World Renewable Energy Congress,* Abu Dhabi, United Arab Emirates, 2010. [Google Scholar]

[16] M.D. Islam et al., "Measurement of Solar Energy Radiation in Abu Dhabi, UAE," *Applied Energy,* vol. 86, no. 4, pp. 511-515, 2009. [CrossRef] [Google Scholar] [Publisher Link]

[17] A. Khalil, and A. Alnajjar, "Experimental and Theoretical Investigation of Global and Diffuse Solar Radiation in the United Arab Emirates," *Renewable Energy*, vol. 6, pp. 537-543, 1995. [CrossRef] [Google Scholar] [Publisher Link]

[18] Matthew Lave, and Jan Kleissl, "Optimum Fixed Orientations and Benefits of Tracking for Capturing Solar Radiation in the Continental United States," *Renewable Energy*, vol. 36, no. 3, pp. 1145-1152, 2011. [CrossRef] [Google Scholar] [Publisher Link]

[19] K.K. Gopinathan, "Optimization of Tilt Angle of Solar Collectors for Maximum Irradiation on Sloping Surfaces," *International Journal of Solar Energy*, vol. 10, no. 1-2, pp. 51-61, 1991. [CrossRef] [Google Scholar] [Publisher Link]